4018–4029 *Nucleic Acids Research, 2007, Vol. 35, No. 12* *Published online 6 June 2007*
doi:10.1093/nar/gkm356

Functional genetic selection of Helix 66 in *Escherichia coli* 23S rRNA identified the eukaryotic-binding sequence for ribosomal protein L2

Kei Kitahara, Akimasa Kajiura, Neuza Satomi Sato and Tsutomu Suzuki*

Department of Chemistry and Biotechnology, Graduate School of Engineering, University of Tokyo, 7-3-1 Hongo, Bunkyo-ku, Tokyo 113-8656, Japan

Received March 29, 2007; Revised and Accepted April 23, 2007

ABSTRACT

Ribosomal protein L2 is a highly conserved primary 23S rRNA-binding protein. L2 specifically recognizes the internal bulge sequence in Helix 66 (H66) of 23S rRNA and is localized to the intersubunit space through formation of bridge B7b with 16S rRNA. The L2-binding site in H66 is highly conserved in prokaryotic ribosomes, whereas the corresponding site in eukaryotic ribosomes has evolved into distinct classes of sequences. We performed a systematic genetic selection of randomized rRNA sequences in *Escherichia coli*, and isolated 20 functional variants of the L2-binding site. The isolated variants consisted of eukaryotic sequences, in addition to prokaryotic sequences. These results suggest that L2/L8e does not recognize a specific base sequence of H66, but rather a characteristic architecture of H66. The growth phenotype of the isolated variants correlated well with their ability of subunit association. Upon continuous cultivation of a deleterious variant, we isolated two spontaneous mutations within domain IV of 23S rRNA that compensated for its weak subunit association, and alleviated its growth defect, implying that functional interactions between intersubunit bridges compensate ribosomal function.

INTRODUCTION

Ribosomes are universally conserved ribonucleoproteins that translate genetic information contained in mRNAs into proteins. In conjunction with ribosomal proteins (r-proteins), rRNAs form the basic structure of the ribosome, and have a crucial role in the fundamental process of protein biosynthesis. Recent structural studies of ribosomal subunits, and the 70S ribosomes, revealed that the functional cores for decoding and peptide-bond formation consist entirely of rRNAs (1–7). The architecture of rRNA diversifies among organisms. In mammalian mitochondria, the lengths of the rRNAs are approximately half that of prokaryotic rRNAs (8,9). Large segments of missing rRNA are replaced by enlarged r-proteins and other mitochondria-specific proteins (10–12). In contrast, eukaryotic ribosomes contain elongated rRNAs, with several insertion sequences, and increased numbers of r-proteins (13). While the architecture of rRNAs might have co-evolved with r-proteins, the fundamental structure and function of ribosomes is preserved in all domains of life. Variation in the RNA-to-protein ratio in ribosomes from various organisms indicates that some structural/functional flexibility between RNA and protein is permissible in the architecture of the ribonucleoproteins. However, the functional domains in rRNAs and several r-proteins are extensively conserved in all living organisms and organella.

Structural analysis of the ribosomes revealed that most of the r-proteins consist of globular domains with unstructured extensions that weave into the interior of the rRNA structure, such that they fill the gaps among the rRNA helices, and play important roles in maintaining the ribosome as a functional molecular machine (1). The roles of r-proteins in the assembly of the ribosomal subunits have been extensively studied using bacterial ribosomes (14,15). The r-proteins, such as L2, L3 and L24, are primary RNA-binding proteins that directly recognize naked 23S rRNAs (16,17). These proteins are thought to bind to their binding sites during transcription of rRNAs, and play important roles in ribosome assembly.

*To whom correspondence should be addressed. Tel: +81 3 58418752; Fax: +81 3 38160106; Email: ts@chembio.t.u-tokyo.ac.jp
Present address:
Neuza Satomi Sato, Institute Adolfo Lutz, Av. Dr. Arnaldo 355 10th floor, 01246-902 Sao Paulo, SP, Brazil.

The rRNA sequences that mediate the interaction with essential r-proteins may have evolved in different organisms without the loss of binding capability.

L2 is a highly conserved r-protein, and the largest in the 50S subunit. Because of its functional importance and degree of conservation, L2 is considered to be one of the most evolutionarily ancient r-proteins (18). Structural analysis of the RNA-binding domain (RBD) of L2 revealed that it has two motifs that are homologous to the oligonucleotide–oligosaccharide binding (OB) fold, and the Src homology 3 (SH3)-like barrel, structures that are often found in RNA- or DNA-binding proteins (19). The primary L2-binding site has been biochemically characterized by footprinting and cross-linking experiments (20,21), and maps to a highly conserved stem-loop structure of H66 [nucleotide positions (np.) 1792–1827] in domain IV of 23S rRNA. In crystal structures of ribosomes, the globular RBD of L2 binds an internal bulge structure (np. 1799–1800 and 1817–1820) of H66, and is located in the intersubunit space of the 50S subunit (1,2). The solvent-exposed surface of the RBD makes molecular contacts with helices 23 and 24 in the 16S rRNA to form bridge B7b (5–7). The amino (N)- and carboxy (C)-terminal extensions of L2 are proximal to the peptidyl-transferase center in the 23S rRNA (1,2,22). Although it is established that the peptidyl-transferase center consists of rRNA, L2 together with L3 are required for efficient peptide-bond formation (23–25). The multifunctional nature of L2 was revealed in experiments by Diedrich *et al.* (26), using reconstituted 50S subunits lacking L2, in which it was demonstrated that L2 is involved in the association of the ribosomal subunits, tRNA binding to the A- and P-sites, and peptide-bond formation. An *in vivo* replacement study showed that eukaryotic L2 (L8e), or archaeal L2 counterparts, can replace *Escherichia coli* L2 and form hybrid ribosomes, and that the hybrid ribosomes are translationally active and incorporated into polysomes (27).

According to phylogenetic analysis of rRNAs from all living organisms, there are two distinct classes of L2-binding sites in H66 (see Figure 2A and B) (28)(www.rna.icmb.utexas.edu). In the crystal structures of bacterial ribosomes, a characteristic base-triple composed of C1800, G1817 and A1819 is visible in the L2-binding site of H66 (see Figure 1C) (1,5). In addition, a G1799·U1818 pair also stacks to this base-triple, and participates in a hydrogen (H)-bond network to form a core structure in this region. This characteristic core structure of the L2-binding site appears to induce a kinked conformation of H66 (see Figure 4A). This type of base-triple, designated as class I binding site, is conserved in bacteria, archea, mitochondria and chloroplasts. In eukaryotic rRNAs, the corresponding bases are replaced by A1800, U1817 and A1819 (*E. coli* numbering). Assuming that eukaryotic L2/L8e-binding sites also have a similar structure as the class I binding site, these three bases are likely to form a characteristic base-triple (Figure 2B), which is designated as class II binding site (see Figure 2B). The class II binding site is highly conserved in eukaryotic rRNAs, while all bacteria-type ribosomes have the class I binding site. Since L8e can replace bacterial L2 in *E. coli* cell, these distinct classes of sequences appear to provide functionally similar binding sites for L2/L8e proteins.

To investigate the functional relationship between the two classes of L2/L8e-binding sites in H66, we employed a genetic system which we have termed systematic selection of functional sequences by enforced replacement (SSER) (29). This method allowed us to identify residues absolutely essential for ribosome function in *E. coli* cells from a randomized rRNA library. Previously, we used this approach to analyze the peptidyl-transferase center (29) and the conserved loop sequence of H69 (30). For the current analysis, a library was constructed by complete randomization of the internal bulge sequence in H66 (Figure 1B), and then subjected to SSER. The selected variants contained naturally occurring rRNA sequences from other organisms, as well as unnatural but nonetheless functional sequences. The results of this study revealed the architecture of the L2-binding site, and provided insight into the evolution of the L2–H66 interaction. In addition, genetic analysis of a ribosome variant indicated that functional interactions between intersubunit bridges could compensate for defective ribosomal function.

MATERIALS AND METHODS

Bacterial strains, plasmids and cultivation

Escherichia coli Δ7p*rrn* strain TA542 (Δ*rrnE* Δ*rrnB* Δ*rrnA* Δ*rrnH* Δ*rrnG*::*cat* Δ*rrnC*::*cat* Δ*rrnD*::*cat* Δ*recA56*/pTRNA66 pHKrrnC) (31) was kindly provided by Dr Catharine L. Squires (Tufts University). The rescue plasmid pRB101 was constructed by introducing the *SacB* gene and the *rrnB* operon into pMW118 (Amp^r, pSC101 ori) (Nippon gene). The plasmid pRB102 was constructed from pMW218 (Km^r, pSC101 ori) (Nippon gene) by insertion of the *rrnB* operon. The plasmid pHKrrnC in strain TA542 was replaced by pRB101 to generate strain NT101, which was used as the host cell for SSER. Cells were grown at 37°C in 2× Luria–Bertani medium (2× LB, 2% tryptone, 1% yeast extract and 1% NaCl); for solid medium, 1.5% agar was added. Antibiotics were added at the following concentrations, when required: 40 μg/ml spectinomycin (Spc), 100 μg/ml ampicillin (Amp) and 50 μg/ml kanamycin (Km). To induce plasmid replacement in strain NT101, 5% sucrose was added to the LB medium. Doubling time of NT102 variants were determined by measuring the optical density at 600 nm every 15 min using a plate reader (Molecular Devices, Inc.)

Construction of plasmids with shortened H66 of 23S rRNA

The template plasmid pRB102 was hyper-methylated by the DNA methyltransferases M-*Alu* I, M-*Hae* III and M-*Hpa* II (NEB), as previously described (29), and then subjected to Quik-Change site-directed mutagenesis (Stratagene), according to manufacturer's instructions, using the following sets of primers: 5′-cacagcactgtgc aaacacgagtggacgtatacggtgtg-3′ (forward) and 5′-cacacc gtatacgtccactcgtgtttgcacagtgctgtg-3′ (reverse) for H66d2; 5′-aacacagcactgtgcaaacacgtggacgtatacggtgtgacgcctgc-3′

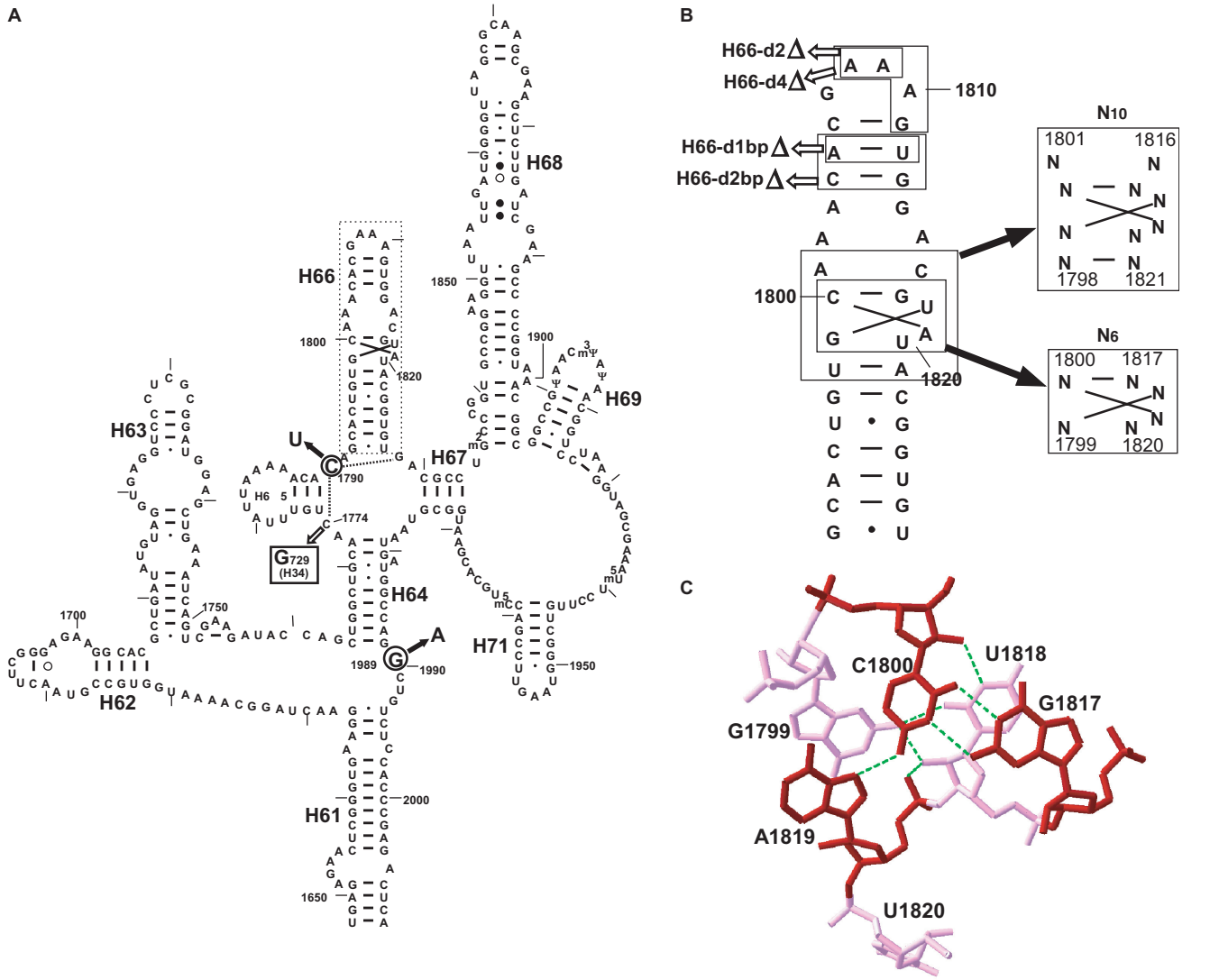

Figure 1. Secondary structure of domain IV of *E. coli* 23S rRNA. (**A**) H66 is boxed in a dotted line. Bars indicate Watson–Crick-type base pairs, black dots indicate wobble base pairs. Non-canonical base pairs are shown in circles. Bases positions selected as compensatory mutations are circled, with the mutation indicated by an arrow. (**B**) Stem loop sequence of H66. The sequences randomized for SSER are boxed. Deletion mutations tested in this study are also indicated. (**C**) Tertiary structure of the internal bulge region (N_6) of H66. The structure of the base-triple, composed of C1800, G1817 and A1819, is shown in red. The other three bases that form the core structure are shown in pink. H-bonds are indicated by dotted lines. Coordinates were obtained from 2AW4 (5).

(forward) and 5′-cgtcacaccgtatacgtccacgtgtttgcacagtgctgtg ttttaataaac-3′ (reverse) for H66d4; 5′-aaaacacagcactgtg caaaccgaaagggacgtatacggtgtgacgcctgc-3′ (forward) and 5′-gcgtcacaccgtatacgtccctttcggtttgcacagtgctgtgtttttaataaac-3′ (reverse) for H66d1bp; and 5′-gtttattaaaaacacagcactgtgcaa acgaaaggacgtatacggtgtgacgcc-3′ (forward) and 5′-ggcgtca-caccgtatacgtcctttcgtttgcacagtgctgtgtttttaataaac-3′ (reverse) for H66d2bp. PCR was carried out, and then the reaction mixture was treated with *Dpn* I (New England Biolabs) to digest the template plasmid, and subjected to purification using QIA-Quick column (Qiagen). NT101 was then transformed with the indicated plasmids. Two plasmids with same origin (pRB101 and pRB102 derivative) transiently coexisted in NT101 cells. To eliminate pRB101, transformed colonies were spotted onto LB-plates containing spectinomycin, kanamycin and sucrose to force plasmid replacement. The *sac*B gene of pRB101 is a counter-selectable marker, which is lethal when expressed in the presence of sucrose; thus, cells carrying only pRB102 (NT102 derivatives) are obtained. The pRB102 variants were confirmed by sequencing.

Construction of plasmid library with randomized nucleotides in Helix66

A non-functional variant of pRB102 (pRB102-H66d4) amplified in *E. coli* DH5α was used as a template for generation of the randomized library. pRB102-H66d4 was hyper-methylated by three DNA methyltransferases, as described above. In the first round of PCR, a set of primers [5′-gtggacgtatacggtgtg-3′ (gap-F) and 5′-gtgtttgcacagtgctgtg (gap-R)] complementary to H66 was employed to generate a gapped template. This process

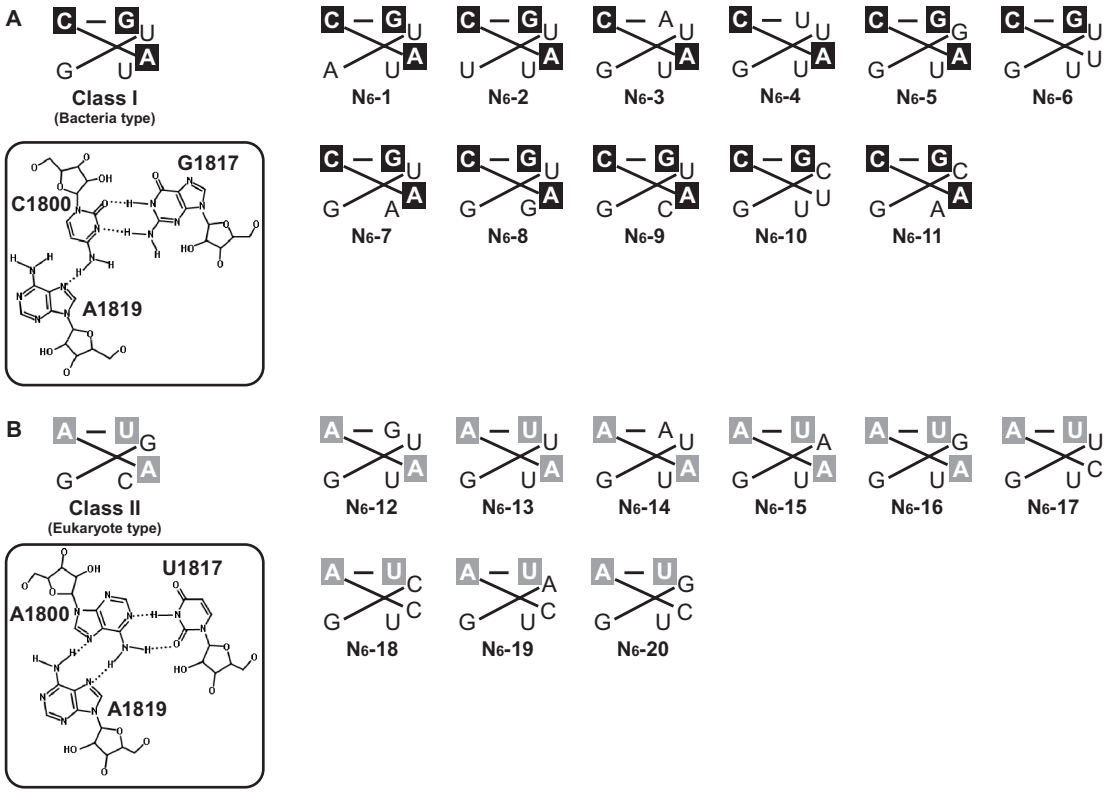

Figure 2. Sequences of the genetically selected functional variants of the N_6-region in H66. (**A**) Secondary structures of the consensus class I L2-binding site, and the 11 class I variants. Consensus base-triple nucleotides (C1800, G1817 and A1819) in each variant are boxed. The inset shows the chemical structure of the base-triple. (**B**) Secondary structures of the consensus class II L2-binding site, and the 9 class II variants. Consensus base-triple nucleotides (A1800, U1817 and A1819) in each variant are boxed. The inset shows the chemical structure of the base-triple.

was required to enhance the efficiency of PCR randomization, and to reduce the background for SSER. Gapped pRB102-H66d4 was then gel-purified and used as the template for the randomized library. To construct the N10 library, a set of primers, N10-F (5′-aacacgaaag tgga NNNNNN cggtgtgacg cctgcccggt gccggaaggt taattg-3′) and N10-R (5′-tccactttcg tgttNNNNca gtgctgtgtt tttaa taaac agttgcag-3′), was employed to randomize 10 bases in the internal bulge region of H66. For the N6 library, a set of primers, N6-F (5′-aacacgaaag tggacNNNNa cggtgtgacg cctgcccggt gccggaaggt taattg-3′) and N6-R (5′-tccactttcg tgtttNNaca gtgctgtgtt tttaataaac agttgcag-3′), was used. The conditions for large-scale PCR to construct the randomized libraries was described previously (29,30). After PCR, the reaction mixture was treated with *Dpn* I (New England Biolabs) and λ exonuclease (New England Biolabs) to digest the template plasmid, then subjected to purification using a QIA-Quick column (Qiagen). The products were then verified by agarose gel electrophoresis. Unbiased distribution of four bases at each position of the randomized region was confirmed by direct sequencing of the plasmid library prior to the selection.

SSER

Details of SSER have been described previously (29,30). NT101 cells were transformed using the randomized library and plated on LB-plates containing Spc/Km. Transformants were picked and suspended in LB broth, then spotted onto LB-plates containing Spc/Km/sucrose to force plasmid replacement. For variants showing a slow growth phenotype, the cell suspension was first spotted and cultivated on LB-plates containing Spc/Km, before transfer to LB-sucrose plates. Sucrose-resistant colonies (NT102 variants) were then cultured in 2× LB broth in preparation for plasmid purification and sequencing. To verify plasmid replacement, each transformant was spotted onto two LB-plates containing Spc/Amp and Spc/Km/sucrose. No growth of the spotted cells on the Amp-plate confirmed complete plasmid replacement. Functional variants were sequenced using an ABI Prism 3100 Genetic Analyzer (Applied biosystems).

Determination of doubling times

To determine the doubling times of NT102 variants, 2 µl of an overnight pre-culture was inoculated into 1 ml of 2× LB medium, then separated into 5 aliquots and plated in a flat-bottomed 96-well microplate (IWAKI). The microplate was incubated at 37°C with vigorous agitation in a Spectramax 190 plate reader (Molecular Device, inc.), and absorbance at 600 nm (OD_{600}) was monitored every 15 min.

Sucrose density gradient analysis

This analysis was based on the procedure described previously (30,32). Briefly, NT102 cells were grown in 50 ml of 2× LB broth containing Spc, Km and sucrose,

in a 500 ml flask with vigorous shaking at 37°C. Cells were harvested by centrifugation when the OD_{600} reached 0.4–0.5. The cell pellet was resuspended in 1 ml of cold RBS buffer (20 mM HEPES–KOH pH 7.6, 6 mM $Mg(OAc)_2$, 30 mM NH_4Cl, 6 mM 2-mercaptoethenol). Cell lysates were prepared by the lysozyme–freeze–thaw method, as described previously (30), and cleared by centrifugation for 15 min at 15 000 r.p.m. at 4°C. The concentration of total RNA in the lysate was estimated by measuring OD_{260}. Fifteen OD units of the lysate was layered on the top of a sucrose gradient (10–40%) prepared in RBS buffer, then separated by ultracentrifugation in a Beckman SW-28 rotor at 20 000 r.p.m. for 14 h at 4°C. Ribosomal subunits in the gradient were fractionated by Piston Gradient Fractionator (BIOCOMP) and monitored at 260 nm using a UV monitor (ATTO AC-5200). The 'assembly ratio' of 50S subunit is defined by calculating molar ratio of total 23S rRNA (and 5S rRNA) against total 16S rRNA in the SDG profiles. The 'association ratio' of 50S to 30S is defined by calculating the portion (%) of 23S rRNA (and 5S rRNA) which is incorporated into the 70S peak.

Generation of revertant strains bearing compensatory mutation

Glycerol stock of variant N_6-16 was pre-cultured in a test tube containing 3 ml of 2× LB medium until full growth (defined as the 0 generation), and then 0.1% (3 µl) of the culture was transferred into three different aliquots of 3 ml of new medium to create three different lineages. After overnight cultivation, each lineage was transferred to a new test tube. Serial passages were repeated for 16 days. After cultivation of 80 and 160 generations (one passage corresponds to approximately 10 generations), doubling time for each lineage was determined. pRB102 derivatives were extracted from each lineage of 80 and 160 generations, and the entire 23S rRNA and most of the 16S rRNA genes were sequenced to identify secondary mutations. To confirm whether the secondary mutations in each lineage functioned as compensatory suppressors for the deleterious effect of the N_6-16 mutation, each of lineage-specific mutation was independently introduced into pRB102 of N_6-16 (0 generation), using the following sets of primers: N_6-16 + C1790U-F (5′-ctgtttattaaaaacatag cactgtgaaaacac-3′) and N_6-16 + C1790U-R (5′-gtgttttca cagtgctatgtttttaataaacag-3′) for the C1790U mutation in N_6-16; C1790U-F (5′-ttaaaaacatagcactgtgcaaacac gaaagtgg-3′) and C1790U-R (5′-gcacagtgctatgtttttaataaa cagttgcag-3′) for the C1790U mutation in wild-type pRB102; and G1989A-F (5′-atggccagactgtctccacccgagact cagtg-3′) and G1989A-R (5′-ggtggagacagtctggccatcat tacgccattcg-3′) for the C1790U mutation in both N6-16 and wild-type pRB102.

RESULTS

Deletion analysis of H66 in 23S rRNA

According to a phylogenetic analysis of rRNAs from various organisms and organelles (28) (www.rna.icmb.utexas.edu), the internal bulge region of H66 (np. 1798–1800 and 1817–1820) is highly conserved. However, the top half of H66 (1801–1816) is not conserved, even in bacteria. In mitochondrial rRNAs, for example, the top half of H66 is nearly truncated. To define the functional L2-binding site, we first examined the effect of deleting bases in the top half of H66. We used the NT101 strain, a derivative of the Δ7*prrn* strain developed in the Squire's laboratory to test the function of rRNAs with deletions. NT101 contains the rescue plasmid pRB101 (Amp^r) carrying both the *rrnB* operon and the *sacB* gene, which produces toxic products in the presence of sucrose. We introduced a second plasmid pRB102 (Km^r) carrying the *rrnB* with deletion in H66. A two-bases deletion (H66-d2) in the H66 loop was introduced into pRB102 (Figure 1B), which then transformed *E. coli* strain NT101, and a functional transformant (H66-d2) was obtained following selection on sucrose plates. Similarly, a one-basepair deletion (ΔA1805·U1812) also yielded a functional variant (H66-d1bp). However, we failed to obtain variants carrying a four-bases deletion (ΔA1808-G1811) in the loop, or a two-basepairs deletion (ΔA1805·U1812/ ΔC1804·G1813), indicating that large deletions in H66 are not tolerated. Thus, we did not test additional variants using this approach. The growth rate of the functional variants (H66-d2 and H66-d1bp) was measured as an estimate of ribosomal activity (Table 1), and we found that small deletions in the top half of H66 resulted in a slight reduction of growth rate.

Comprehensive genetic selection of the L2-binding site in H66

To investigate the functional importance of the highly conserved bulge region of H66 in the 23S rRNA, we employed a novel genetic method developed in our lab, SSER (29). This system allows the rapid identification of functional sequences from a library of randomized sequences. Based on crystal structure of the *E. coli* 70S ribosome (5), ten conserved nucleotides (1798–1801 and 1816–1821) in the bulge region of H66 were chosen for randomization, as they represented the potential binding site for L2 (Figure 1B). The ten bases in H66 were completely randomized using a PCR-based method, generating a pRB102 library with 1 048 576 sequence variations (N_{10} library) (Figure 1B). We employed a non-functional plasmid variant, H66-d4, amplified in *E. coli* DH5α as the template for PCR-randomization, rather than wild-type pRB102, to exclude the possibility of wild-type sequences being generated and isolated during the selection process. We then carried out a large-scale transformation of *E. coli* strain NT101 with the randomized library, and transformants were selected based on

Table 1. Growth rate of *E. coli* strains bearing ribosome variants

Strains	Doubling time (min)	RGR (%)
Wt	50.4 ± 1.5	100
H66d2	58.9 ± 1.6	86
H66d4	ND	ND
H66d1bp	70.1 ± 1.2	72
H66d2bp	ND	ND

kanamycin resistance. If the sequence of the incorporated plasmid was toxic, showing a dominant lethal phenotype, the transformant was eliminated in this step. As L2 is an essential primary rRNA-binding protein, it is likely that most of the sequences in the library were excluded during this step. The kanamycin-resistant transformants showed different colony sizes (data not shown), indicating that the cells contained a sequence that resulted in altered ribosomal activity. At this stage, two incompatible plasmids, pRB101 (Amp^r) and pRB102 (Km^r), transiently coexisted in the *E. coli* transformants. To drive plasmid replacement, we took advantage of the counter selection system in which *sacB* gene on pRB101 produces toxic products in the presence of sucrose. Each cell was picked and spotted onto selection plates containing kanamycin and sucrose. If the incorporated pRB102 plasmid had a functional sequence for ribosomal activity, it rapidly eliminated the pRB101 rescue plasmid, thus yielding sucrose-resistant cells (NT102 derivatives). Besides, if the incorporated plasmid had a non-functional or very weak functional sequence for ribosomal activity, the rescue plasmid (pRB101) could not be replaced by the introduced plasmid and the transformant became sensitive to sucrose due to the *sacB* gene.

Most likely due to the vast number of sequence variations in the N_{10} library and the functional importance in the randomized region, we obtained only 15 sucrose-resistant clones, from approximately 22 500 kanamycin-resistant colonies. Complete plasmid replacement of the selected variants was verified by their inability to grow in the presence of ampicillin. Functional plasmids were sequenced, resulting in the identification of 14 viable sequences from the N_{10} library (Table 2). No wild-type sequences were isolated. The variants had one-, two- or three-nucleotide changes in the randomized region, as compared to the wild-type sequence. While the sequence data provided only limited information, the results indicated that the peripheral four nucleotides (U1798, A1801, C1816 and A1821) are variable, and the internal six nucleotides (1799–1800 and 1817–1820) are less variable. To more precisely define the molecular features of the functional L2-binding site, we focused on the internal six nucleotides for another round of SSER.

Table 2. Functional sequences (1798–1801/1816–1821) of H66 of 23S rRNA selected by SSER from an N_{10} randomized rRNA libraries

Clones	Sequences (1798–1801/1816–1821)	Number of isolates
Wt	UGCA/CGUAUA	0
N_{10}-1	AGCA/CGUAUA	1
N_{10}-2	UGCC/CGUAUA	1
N_{10}-3	UGCU/CGUAUA	1
N_{10}-4	UGCA/CAUAUA	1
N_{10}-5	GGCC/CGUAUA	2
N_{10}-6	CGCC/CGUAUA	1
N_{10}-7	CGCG/CGUAUA	1
N_{10}-8	UACC/CGUAUA	1
N_{10}-9	UGAC/CGUAUA	1
N_{10}-10	UGAU/CGUAUA	1
N_{10}-11	UGCA/CGUAAC	1
N_{10}-12	UGCA/CGUACU	1
N_{10}-13	UGCA/GGUGUA	1
N_{10}-14	UGCC/AGUAUG	1

The six internal nucleotides (1799–1800 and 1817–1820) of H66 were completely randomized to construct a pRB102 library with 4096 sequence variations (N_6 library) (Figure 1B). In this round of selection, in order to rescue less than fully functional sequences, primary kanamycin-resistant transformants were cultivated for an additional period of time before counter selection on sucrose plates. We obtained 25 sucrose-resistant colonies, and sequence analysis of the randomized region revealed 21 distinct functional clones, including one with the wild-type sequence (N_6-0) (Table 3). Among them, two variants (N_6-1 and N_6-10) were present twice, and one variant (N_6-2) was present three times. The selected variants had changes of one to four nucleotides compared to the wild-type sequence. These results demonstrated that SSER of the N_6 library successfully identified sufficient number of functional sequences. It is noteworthy that replacement of C1800 by A1800 was functional, in light of the fact that C1800 is completely conserved in bacteria, archaea and chloroplasts. G1799 and U1820 were preferentially selected. Although most of the selected clones contained non-naturally occurring sequences, N_6-0 is a conserved sequence found in bacteria and archaea, and N_6-1 (G1799A) is a natural sequence found in some archaea. Intriguingly, N_6-16 is also a natural sequence found in eukaryotic rRNA (*Protopterus aethiopicus*) (33).

According to their predicted secondary structures, 20 of the selected variants could be clearly divided into two distinct classes, based on the characteristic base-triple in the L2-binding site of H66 (Figure 2A and B). The two classes were characterized by either a C1800- or an A1800-centered base-triple. Eleven variants (N_6-1 to N_6-11) carrying C1800 were categorized as class I, and nine variants (N_6-12 to N_6-20) carrying A1800 were categorized as class II. In class I variants, G1817 in the binding site tended to be co-selected with C1800 (9 variants). Similarly, in the class II binding site, U1817 appeared to be co-selected with A1800 (7 variants). Hence, all variants carried at least two of the three bases of the base-triple. These results indicated that co-variation in the selected variants is required for proper organization of the L2-binding site.

Deficiency in subunit association in ribosomes with altered L2-binding sites

To examine the growth phenotype of each variant selected from the N_6 library, we generated new constructs of each of the variants, to avoid the generation of secondary mutations at unexpected positions or compensatory mutations during selection and sub-culturing. The growth rate of each variant was measured as an estimate of ribosomal activity (Table 3). We observed a weak relationship between the number of mutations and doubling times. Of the class I variants, N_6-4, carrying a U1817 substitution, showed a reduced growth phenotype. In this variant, U1817 is unable to form a base-triple with C1800 and A1819. N_6-11, carrying C1818 and A1820

substitutions, also showed a growth defect, whereas N_6-7, carrying a single A1820 substitution, did not. Thus, the slow growth of N_6-11 likely originated from the combination of C1818 and A1820. Compared to the class I variants, the average growth rate of the class II variants was decreased. N_6-16, which contained a naturally occurring eukaryotic L2-binding site, exhibited the most severe phenotype. There were three class II variants, N_6-13, N_6-15 and N_6-16, which had a complete class II base-triple, but different bases at position 1818. N_6-13, carrying a U at position 1818, showed the highest growth rate of the class II variants, indicating that the growth of these variants was modulated by the specificity of position 1818.

The growth defects of each variant indicated that they had decreased functionality of their ribosomes. Since L2 is known to participate in subunit association through bridge B7b, we next examined the efficiency of subunit association in eight of the rRNA variants (N_6-0, N_6-4, N_6-9, N_6-11, N_6-13, N_6-16, N_6-19 and N_6-20), using sucrose density gradient (SDG) centrifugation (Figure 3A). The association ratio [(50S incorporated into 70S)/(total 50S)] and the assembly ratio [(total 23S rRNA)/(total 16S rRNA)] of the 50S subunit for each variant were calculated from the SDG profile (Table 3). We observed little influence of sequence variation on the assembly ratio of the 50S subunit (Figure 3A and Table 3). In wild-type ribosomes, 71.6% of intact 50S subunits were incorporated into tightly coupled 70S ribosomes (TC) in the presence of 6 mM magnesium (Mg^{2+}). Similar SDG profiles, indicating normal subunit association, were observed in ribosome variants N_6-9, N_6-13 and N_6-19, variants that also showed a healthy growth phenotype. In contrast, the SDG profiles of ribosome variants with slow growth phenotypes revealed apparently lower TC ratios (Figure 3A). In N_6-4 and N_6-20 ribosomes, 45.1 and 47.4% of the 50S subunits were incorporated into TC, respectively. In addition, two variants with lower growth rates, N_6-11 and N_6-16, showed a marked reduction in TC formation, with association ratios of 24.6 and 23.1%, respectively. Thus, the slow growth phenotype of H66 variants correlated well with weak subunit association.

The deleterious effect of L2-binding site mutations is suppressed by compensatory mutations in domain IV of 23S rRNA

To identify genetic interactions between the L2-binding site and other sites in the rRNA, we attempted to isolate revertants of the variant with the most severe phenotype, N_6-16, whose doubling time was 97.7 min (Table 3). N_6-16 cells were divided into three lineages and cultivated for 16 days, with repeated serial passage into new medium.

Table 3. Functional sequences (1799–1800/1817–1820) and growth rates of variants of H66 of 23S rRNA selected by SSER from an N_6 randomized rRNA library

Clones	Sequences (1799–1800/1817–1820)	Doubling time (min)	RGR (%)	Number of isolates	Conservation	Association	Assembly
N_6-0(Wt)	GC/GUAU	50.4 ± 1.5	100	1	B,A	71.6	1.16
N_6-1	AC/GUAU	59.2 ± 1.2	85	2			
N_6-2	UC/GUAU	59.6 ± 2.2	85	3			
N_6-3	GC/AUAU	52.4 ± 0.5	96	1			
N_6-4	GC/UUAU	77.0 ± 1.8	65	1		45.1	0.96
N_6-5	GC/GGAU	52.0 ± 1.5	97	1			
N_6-6	GC/GUUU	53.4 ± 1.4	94	1			
N_6-7	GC/GUAA	52.6 ± 1.1	96	1			
N_6-8	GC/GUAG	51.8 ± 3.0	97	1			
N_6-9	GC/GUAC	50.1 ± 0.5	101	1	A	74.3	1.08
N_6-10	GC/GCUU	60.8 ± 1.3	83	2			
N_6-11	GC/GCAA	79.6 ± 2.6	63	1		24.6	1.08
N_6-12	GA/GUAU	63.7 ± 1.4	79	1			
N_6-13	GA/UUAU	55.4 ± 2.3	91	1		76.3	1.12
N_6-14	GA/AUAU	65.9 ± 5.7	76	1			
N_6-15	GA/UAAU	65.7 ± 0.7	77	1			
N_6-16	GA/UGAU	97.7 ± 4.6	52	1	E	23.1	1.29
N_6-17	GA/UUCU	60.8 ± 2.2	83	1			
N_6-18	GA/UCCU	58.5 ± 0.8	86	1			
N_6-19	GA/UACU	59.8 ± 3.1	84	1		71.2	1.11
N_6-20	GA/UGCU	72.2 ± 1.0	70	1		47.4	1.07
Consensus	DM/DNHN						
N_6-16(rev1)		45.7 ± 0.9	110				
N_6-16(rev2)		56.0 ± 1.3	90				
N_6-16(rev3)		50.3 ± 1.2	100				
N_6-16+C1790U		52.6 ± 1.7	96			65.4	1.16
N_6-16 + G1989A		58.5 ± 3.6	86			65.5	1.2
C1790U		51.2 ± 4.8	98			64.2	1.29
G1989A		51.0 ± 2.5	99			60.1	1.27

Values for the association and assembly of ribosomes were calculated as described in Materials and Methods section. Relative growth rate (RGR%) for each variant is indicated. The SD values of wild-type association and assembly are 4.94 and 0.031, respectively. The nomenclature for mixed bases used in this study obey rules previously established (44), in which M indicates A or C, D indicates all bases except C, H indicates all bases except G, and N indicates all bases (A, U, G or C).

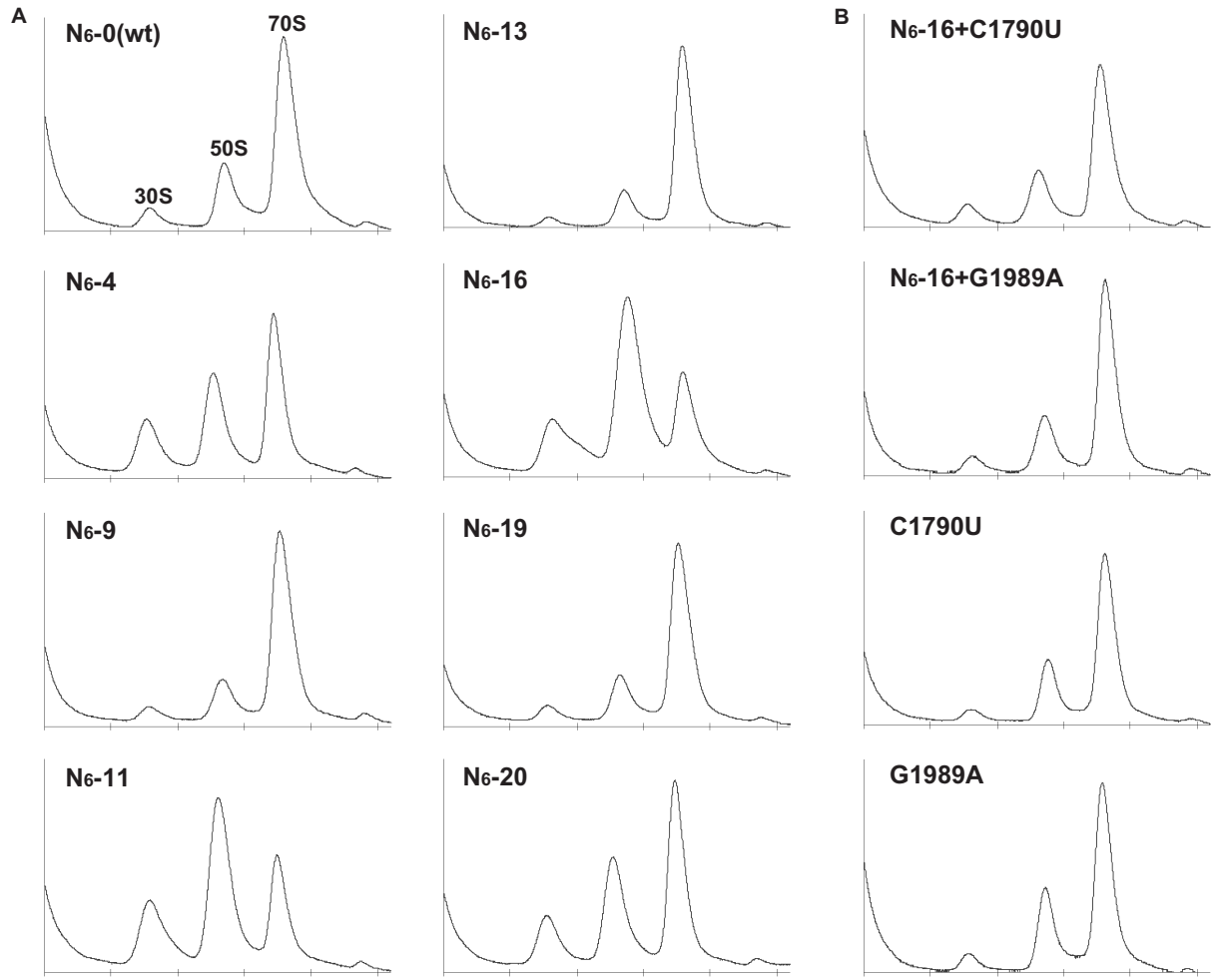

Figure 3. Subunit association profiles of the H66 variants. (A) Sucrose density gradient centrifugation profiles of wild-type ribosomes, and the H66 variants, in the presence of 6 mM Mg^{2+}. Peak assignments for the 70S, 50S and 30S subunits are indicated in the wild-type profile. (**B**) Sucrose density gradient centrifugation profiles of the N_6-16 revertants, with the indicated mutations (top two panels), and wild-type ribosomes carrying the indicated point mutation (bottom two panels).

We succeeded in isolating three independent populations in which the growth rate was significantly improved: revertant 1 (doubling time 45.7 min), revertant 2 (doubling time 56.0 min) and revertant 3 (doubling time 50.3 min). The doubling time of revertant 1 was faster than that of wild type (50.4 min). We observed an increased amount of pRB102 plasmid extracted from this population (data not shown), indicating that increased plasmid copy number and general adaptation to the medium during cultivation accounted for the growth phenotype. We sequenced each pRB102 revertant and identified three different mutations that appeared to be responsible for the compensatory effect on the N_6-16 L2-binding site mutant. In revertant 1, we identified a C1790U mutation. This position is approximately ten bases upstream of the N_6 region. Revertant 2 had a G1818U mutation, which is within the N_6 region, changing the N_6-16 sequence to that of N_6-13, which had a normal growth phenotype. Revertant 3 had a G1989A mutation, at the position located approximately 170 bases downstream of the N_6 region. To confirm that the C1790U and G1989A mutations functioned as suppressors for the deleterious effect of the L2-binding site mutation in N_6-16, each of the compensatory mutations was reconstituted into a derivative of pRB102 obtained from ancestral N_6-16 cells. NT101 cells were transformed with each of the compensatory mutant plasmids to obtain two NT102 derivatives: N_6-16 + C1790U, and N_6-16 + G1989A. As shown in Table 3, the growth rates of these strains were significantly increased (52.6 and 58.5 min, respectively). Thus, we confirmed that the C1790U and G1989A mutations suppress the deleterious effect of the L2-binding site mutation of N_6-16. Furthermore, SDG analyses revealed that both N_6-16 + C1790U and N_6-16 + G1989A had significantly improved association ratios, ranging from 23.1 to ~65% (Table 3 and Figure 3B). These results suggested that both mutations are able to suppress the defect in subunit association caused by mutation of the

L2-binding site. In control experiments, to estimate the effect of the C1790U or G1989A mutation in a wild-type background, two NT102 derivatives with a single mutation (either C1790U or G1989A) were constructed. Both strains showed normal growth rates (Table 3). The C1790U mutant showed a similar subunit association ratio (64.2%) to N_6-16 + C1790U, while the G1989A mutant showed a slight reduction in subunit association (60.1%), compared to N_6-16 + G1989A (Table 3 and Figure 3B). These results suggested that a C1790U or G1989A mutation alone does not exert a positive effect on the basal activity of 23S rRNA.

DISCUSSION

We carried out a functional genetic selection of 23 rRNA L2-binding site variants using an advanced genetic selection system developed in our lab, termed SSER (29), allowing the identification of sequences that are essential for ribosome function from a randomized rRNA library in *E. coli*. Using SSER, we isolated functional sequences from independent colonies, eliminating competition against other variants for survival. As long as sufficient numbers of transformants are obtained, this method can be used to test the functionality of all possible sequences, including wild-type sequences, and naturally occurring sequences found in other organisms, as well as unnatural but functional sequences that have not emerged during the process of evolution. Thus, SSER permits completely neutral genetic selection of functional sequences, as it excludes researcher's arbitrariness and bias. From the selected sequences, we can identify *bona fide* sequences that would not be available from a phylogenetic comparison of rRNA sequences. In addition, SSER can identify distinct classes of functional sequences with low homology to each other, as was the case for the L2-binding sites identified in this study, whereas other approaches using conventional site-directed mutagenesis may miss this distinction.

Since SSER is based on the replacement of the *rrn*-operon, the selection of rRNA sequences required for translating the entire proteome of *E. coli* is stringent. Moreover, as limited numbers of transformants are available due to practical experimental designs, the size of the randomized region for SSER was restricted. In previous studies, we successfully selected functional sequences from an N_6 library (4096 variations) of the 2451-region of the peptidyl-transferase center (29), and from an N_7 library (16 384 variations) of the conserved loop of H69 (30). In the current study, we initially selected functional sequences of a 10-base region in the L2-binding site, using a randomized plasmid library containing 1 048 576 sequence variations (N_{10} library). To date, this is the largest rRNA library used for SSER. Although we successfully obtained 14 functional sequences, from approximately 22 500 colonies in the initial screen, this experiment gave us limited information on the L2-binding site, and as such, was not practical or effective. For SSER to be effective, we had to design an appropriately sized library, taking into consideration the functional importance of the target region.

From an N_6 library of the internal six nucleotides of the L2-binding site, we successfully isolated 20 functional variations as well as the wild-type sequence. Variants could be divided into 12 class I sequences, and 9 class II sequences, even though this region is a highly conserved site in all living organisms. Since L2 is a primary binding protein in the biogenesis of the 50S subunit (16,17), we explored whether alterations in the binding site had a deleterious effect on 50S assembly and/or incorporation of L2 into 50S particles. We found that no variants showed decreased assembly ratio as calculated from SDG profiles (Table 3). In addition, the stoichiometry of L2 in the isolated ribosomes from the slow growth variants was examined by SDS-PAGE, and we found no evidence of decreased amounts of L2 in any of the variants (data not shown). During SSER, rRNA variants which do not have a strong binding affinity for L2 are eliminated as dominant lethal or non-functional mutants. An intriguing finding of this study is that the sequence of one of the L2-binding site variants corresponded to the eukaryotic class of L2-binding site. Among the 9 class II variants, N_6-16 was a naturally occurring sequence found in a eukaryotic rRNA (*Protopterus aethiopicus*) (33). This finding demonstrates that L2 can recognize class II binding sites in *E. coli* ribosomes. Cytosine or adenosine at position 1800 was selected as an essential base; it acts as a central base required to form the characteristic base-triple in the L2-binding site. Interestingly, G1817 and U1817 were preferentially selected with C1800 and A1800, respectively, indicating that there is specific co-variation in the bases at positions 1800 and 1817. When C1800 was replaced with A1800 (as in variant N_6-12), the doubling time of the variant decreased to 63.7 min. In addition, a single G1817U mutation (N_6-4) also resulted in a reduced growth rate (77.0 min). However, when these mutations were introduced simultaneously (N_6-13), the growth rate was improved (55.4 min), demonstrating the functional interaction of these two positions, consistent with the idea that the characteristic base-triple is required for proper organization of the L2-binding site. The crystal structures of eukaryotic ribosomes at atomic-scale resolution will help illuminate the structure of the class II base-triple and the mechanism of recognition by L8e.

Typically, ribosomal proteins interact indirectly with rRNAs through salt-bridges between positively charged residues on the protein and phosphate oxygen atoms on the rRNA (34–37). According to this mechanism, proteins recognize specific surface features of regular helical segments interrupted by irregularities, such as non-canonical base pairs, base-triples, single bulged nucleotides and small internal loops (38,39). In the case of the L2–H66 interaction, the globular RBD of L2 mainly recognizes a backbone structure of the internal bulge region in H66. In the crystal structure of the *E. coli* 70S ribosome (5), no base-specific interactions between the RBD of L2 and the N_6 region were observed. This binding mechanism is consistent with a common feature of RNA–protein interactions in the ribosome, in which base-specific interactions are less important. Also, the recognition of

specific structural features of the RNA by L2 can explain the finding that two distinct classes of L2-binding sites were selected from the randomized library; each one might form a similar tertiary structure that is recognized by L2/L8e proteins. From an evolutionary viewpoint, it is plausible that rRNAs originally provided two classes of aptamers for the globular RBD of L2 proteins. When the ancestral species of eukaryotes arose from prokaryotes, it is possible that the class II binding site was selected incidentally, rather than co-evolving with the L2/L8e protein.

SDG analysis revealed a good correlation between the growth phenotype and subunit association of each variant. As the globular domain of L2 is located at the intersubunit surface, and forms bridge B7b with helices 23 and 24 of 16S rRNA, it is likely that functional variations in the L2-binding site affect the configuration of L2, leading to weakening of bridge B7b. The N-terminal extension of L2 directly interacts with the base region of H34 in domain II of the 23S rRNA, and the tip of H34 directly interacts with S15 in the 30S subunit to form bridge B4. It is known that bridge B4 is an important functional site for subunit association (40,41). Previously, we showed that even a short deletion in H34 has a great effect on subunit association (32). The N-terminal extension of L2 could be affected by alterations in the L2-binding site, which modulates the relative orientation of the H34 tip and S15. In support of this, deleterious ribosome variants with altered L2-binding sites showed defective subunit association. We obtained two revertants of variant N_6-16, in which the weak subunit association was recovered. Each revertant contained a point mutation in domain IV of the 23S rRNA. Revertant 1 had a C1790U mutation in the base region of H66 (Figure 1A). In the crystal structure of the *E. coli* 70S ribosome (Figure 4A and B), C1790 forms a hydrogen bond with C1774, which base-pairs with G729 of H34 in domain II of the 23S rRNA. Mutation of C1790U would affect the relative configuration of H34 and H66, through the U1790–C1774 interaction. As a single mutation C1790U in the background of wild-type rRNA had little effect on the ribosome, C1790U must have a specific compensatory effect on the defective subunit association of the N_6-16 variant. Revertant 3 had a G1989A mutation, which is located near H64 (Figure 1A). Since G1989 directly interacts with positions 1474–1476 in helix 44 of the 16S rRNA to form bridge B5 (42), it is possible that the G1989A mutation modulates bridge B5, thus compensating for defective subunit association. As a single mutation in the background of wild-type rRNA, G1989A caused a slight reduction of subunit association, indicating that the G1989A mutation in N_6-16 had a modulatory function, perhaps in fine-tuning intersubunit association. Together, these results suggest that a variety of mechanisms of compensation of defective subunit association are possible by modulation of intersubunit bridges.

The reduction in growth rate caused by antibiotic resistance can be compensated by various mutations, most of which reside in r-proteins. For example, a mutation in the S12 gene, which confers resistance to streptomycin and causes growth reduction, is compensated by second site

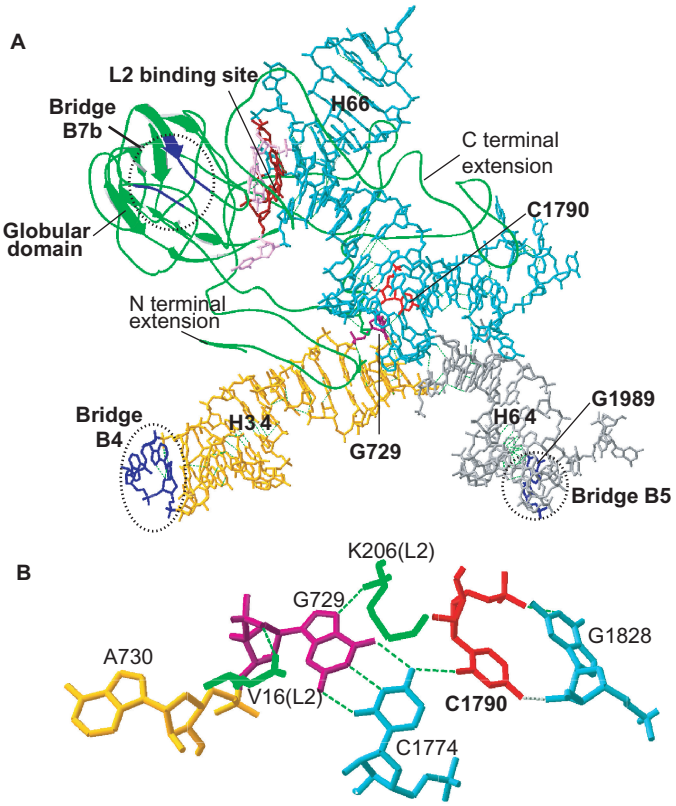

Figure 4. Molecular interactions between L2 and H66 in *E. coli* 50S subunit. (**A**) Structures of H66 (cyan), H64 (gray) and H34 (orange) interacting with L2 (green). The L2-binding site (N_6 region) is colored in red and pink, as shown in Figure 1C. The positions of G729, C1790 and G1989 are indicated. The intersubunit bridges B7b (L2), B4 (H34) and B5 (H64) are shown in blue. Coordinates were obtained from 2AW4 (5). (**B**) Enlarged view of the H34–H66 interaction through G729–C1774 pairing. C1790 and two residues (K206 and V16) in L2 are also involved in this interaction.

mutations in various r-proteins, such as S4, S5, S12 and L19 (43). Although these are many examples of protein–protein compensation, few examples of RNA–RNA compensation have been reported. The lack of data may be due to the lack of a suitable experimental system for this type of analysis. As described in this study, our selection system can readily provide vast numbers of functional rRNA mutants with severe growth phenotypes. In addition, we were able to successfully identify compensatory RNA mutations from revertants of an original rRNA variant. These results, and this type of analysis in general, will help elucidate the many genetic interactions between functional sites in rRNAs, unveiling the ribosomal dynamics at each step of translation.

ACKNOWLEDGEMENTS

We are grateful to the Suzuki lab members for many fruitful discussions and technical advices. We would also like to thank Dr Catherine L. Squires for providing us with valuable strains and plasmids. This work was supported by grants-in-aid for scientific research on priority areas from the Ministry of Education, Science,

Sports and Culture of Japan (to T.S.) and the Human Frontier Science Program (RGY23/2003) (to T.S.). Funding to pay the Open Access publication charges for this article was provided by the Japan Ministry of Education, Science, Sports and Culture.

Conflict of interest statement. None declared.

REFERENCES

1. Ban,N., Nissen,P., Hansen,J., Moore,P.B. and Steitz,T.A. (2000) The complete atomic structure of the large ribosomal subunit at 2.4 Å resolution. *Science*, **289**, 905–920.
2. Harms,J., Schluenzen,F., Zarivach,R., Bashan,A., Gat,S., Agmon,I., Bartels,H., Franceschi,F. and Yonath,A. (2001) High resolution structure of the large ribosomal subunit from a mesophilic eubacterium. *Cell*, **107**, 679–688.
3. Wimberly,B.T., Brodersen,D.E., Clemons,W.M. Jr, Morgan-Warren,R.J., Carter,A.P., Vonrhein,C., Hartsch,T. and Ramakrishnan,V. (2000) Structure of the 30S ribosomal subunit. *Nature*, **407**, 327–339.
4. Schluenzen,F., Tocilj,A., Zarivach,R., Harms,J., Gluehmann,M., Janell,D., Bashan,A., Bartels,H., Agmon,I. *et al.* (2000) Structure of functionally activated small ribosomal subunit at 3.3 angstroms resolution. *Cell*, **102**, 615–623.
5. Schuwirth,B.S., Borovinskaya,M.A., Hau,C.W., Zhang,W., Vila-Sanjurjo,A., Holton,J.M. and Cate,J.H. (2005) Structures of the bacterial ribosome at 3.5 Å resolution. *Science*, **310**, 827–834.
6. Selmer,M., Dunham,C.M., Murphy,, ,, Weixlbaumer,A., Petry,S., Kelley,A.C., Weir,J.R. and Ramakrishnan,V. (2006) Structure of the 70S ribosome complexed with mRNA and tRNA. *Science*, **313**, 1935–1942.
7. Korostelev,A., Trakhanov,S., Laurberg,M. and Noller,H.F. (2006) Crystal structure of a 70S ribosome-tRNA complex reveals functional interactions and rearrangements. *Cell*, **126**, 1065–1077.
8. O'Brien,T.W. (1971) The general occurrence of 55 S ribosomes in mammalian liver mitochondria. *J. Biol. Chem.*, **246**, 3409–3417.
9. Hamilton,M.G. and O'Brien,T.W. (1974) Ultracentrifugal characterization of the mitochondrial ribosome and subribosomal particles of bovine liver: molecular size and composition. *Biochemistry*, **13**, 5400–5403.
10. Suzuki,T., Terasaki,M., Takemoto-Hori,C., Hanada,T., Ueda,T., Wada,A. and Watanabe,K. (2001) Proteomic analysis of the mammalian mitochondrial ribosome. Identification of protein components in the 28 S small subunit. *J. Biol. Chem.*, **276**, 33181–33195.
11. Suzuki,T., Terasaki,M., Takemoto-Hori,C., Hanada,T., Ueda,T., Wada,A. and Watanabe,K. (2001) Structural compensation for the deficit of rRNA with proteins in the mammalian mitochondrial ribosome. Systematic analysis of protein components of the large ribosomal subunit from mammalian mitochondria. *J. Biol. Chem.*, **276**, 21724–21736.
12. Suzuki,T., Ohtsuki,T. and Watanabe,K. (2004) Glimpses of transitions from the RNA world to the RNP world in protein compensation for RNA deficit in animal mitochondrial translation systems. *Endocytobiosis Cell Res.*, **15**, 110–122.
13. Taylor,D., Frank,J. and Kinzy,T. (2006) Structure and Function of the Eukaryotic Ribosome and Elongation Factors. Translational Control in Biology and Medicine. Cold Spring Harbor Laboratory Press, New York, 59–85.
14. Traub,P. and Nomura,M. (1968) Structure and function of E. coli ribosomes. V. Reconstitution of functionally active 30S ribosomal particles from RNA and proteins. *Proc. Natl Acad. Sci. USA*, **59**, 777–784.
15. Nierhaus,K.H. (2004) Ribosome Assembly. Protein Synthesis and Ribosome Structure. Wiley-VCH, Weinheim, 85–105.
16. Nomura,M. and Erdmann,V.A. (1970) Reconstitution of 50S ribosomal subunits from dissociated molecular components. *Nature*, **228**, 744–748.
17. Herold,M. and Nierhaus,K.H. (1987) Incorporation of six additional proteins to complete the assembly map of the 50 S subunit from Escherichia coli ribosomes. *J. Biol. Chem.*, **262**, 8826–8833.
18. Tanaka,I., Nakagawa,A., Nakashima,T., Taniguchi,M., Hosaka,H. and Kimura,M. (2000) Structure and Evolution of the 23S rRNA Binding Domain of Protein L2 The ribosome: Structure, Function, Antibiotics, and Cellular Interactions. ASM Press, Washington, DC, 85–92.
19. Nakagawa,A., Nakashima,T., Taniguchi,M., Hosaka,H., Kimura,M. and Tanaka,I. (1999) The three-dimensional structure of the RNA-binding domain of ribosomal protein L2; a protein at the peptidyl transferase center of the ribosome. *EMBO J.*, **18**, 1459–1467.
20. Gulle,H., Hoppe,E., Osswald,M., Greuer,B., Brimacombe,R. and Stoffler,G. (1988) RNA-protein cross-linking in Escherichia coli 50S ribosomal subunits; determination of sites on 23S RNA that are cross-linked to proteins L2, L4, L24 and L27 by treatment with 2-iminothiolane. *Nucleic Acids Res.*, **16**, 815–832.
21. Egebjerg,J., Christiansen,J. and Garrett,R.A. (1991) Attachment sites of primary binding proteins L1, L2 and L23 on 23 S ribosomal RNA of Escherichia coli. *J. Mol. Biol.*, **222**, 251–264.
22. Nissen,P., Hansen,J., Ban,N., Moore,P.B. and Steitz,T.A. (2000) The structural basis of ribosome activity in peptide bond synthesis. *Science*, **289**, 920–930.
23. Schulze,H. and Nierhaus,K.H. (1982) Minimal set of ribosomal components for reconstitution of the peptidyltransferase activity. *EMBO J.*, **1**, 609–613.
24. Noller,H.F., Hoffarth,V. and Zimniak,L. (1992) Unusual resistance of peptidyl transferase to protein extraction procedures. *Science*, **256**, 1416–1419.
25. Khaitovich,P., Mankin,A.S., Green,R., Lancaster,L. and Noller,H.F. (1999) Characterization of functionally active subribosomal particles from Thermus aquaticus. *Proc. Natl Acad. Sci. USA*, **96**, 85–90.
26. Diedrich,G., Spahn,C.M., Stelzl,U., Schafer,M.A., Wooten,T., Bochkariov,D.E., Cooperman,B.S., Traut,R.R. and Nierhaus,K.H. (2000) Ribosomal protein L2 is involved in the association of the ribosomal subunits, tRNA binding to A and P sites and peptidyl transfer. *EMBO J.*, **19**, 5241–5250.
27. Uhlein,M., Weglohner,W., Urlaub,H. and Wittmann-Liebold,B. (1998) Functional implications of ribosomal protein L2 in protein biosynthesis as shown by in vivo replacement studies. *Biochem. J.*, **331**(Pt 2), 423–430.
28. Gutell,R.R. and Fox,G.E. (1988) A compilation of large subunit RNA sequences presented in a structural format. *Nucleic Acids Res.*, **16**(Suppl), r175–r269.
29. Sato,N.S., Hirabayashi,N., Agmon,I., Yonath,A. and Suzuki,T. (2006) Comprehensive genetic selection revealed essential bases in the peptidyl-transferase center. *Proc. Natl Acad. Sci. USA*, **103**, 15386–15391.
30. Hirabayashi,N., Sato,N.S. and Suzuki,T. (2006) Conserved loop sequence of helix 69 in Escherichia coli 23 S rRNA is involved in A-site tRNA binding and translational fidelity. *J. Biol. Chem.*, **281**, 17203–17211.
31. Asai,T., Zaporojets,D., Squires,C. and Squires,C.L. (1999) An Escherichia coli strain with all chromosomal rRNA operons inactivated: complete exchange of rRNA genes between bacteria. *Proc. Natl Acad. Sci. USA*, **96**, 1971–1976.
32. Komoda,T., Sato,N.S., Phelps,S.S., Namba,N., Joseph,S. and Suzuki,T. (2006) The A-site finger in 23 S rRNA acts as a functional attenuator for translocation. *J. Biol. Chem.*, **281**, 32303–32309.
33. Zardoya,R. and Meyer,A. (1996) Evolutionary relationships of the coelacanth, lungfishes, and tetrapods based on the 28S ribosomal RNA gene. *Proc. Natl Acad. Sci. USA*, **93**, 5449–5454.
34. Conn,G.L., Draper,D.E., Lattman,E.E. and Gittis,A.G. (1999) Crystal structure of a conserved ribosomal protein-RNA complex. *Science*, **284**, 1171–1174.
35. Wimberly,B.T., Guymon,R., McCutcheon,J.P., White,S.W. and Ramakrishnan,V. (1999) A detailed view of a ribosomal active site: the structure of the L11-RNA complex. *Cell*, **97**, 491–502.
36. Allers,J. and Shamoo,Y. (2001) Structure-based analysis of protein-RNA interactions using the program ENTANGLE. *J. Mol. Biol.*, **311**, 75–86.
37. Brodersen,D.E., Clemons,W.M. Jr, Carter,A.P., Wimberly,B.T. and Ramakrishnan,V. (2002) Crystal structure of the 30 S

ribosomal subunit from Thermus thermophilus: structure of the proteins and their interactions with 16 S RNA. *J. Mol. Biol.*, **316**, 725–768.
38. Stern,S., Powers,T., Changchien,L.M. and Noller,H.F. (1989) RNA-protein interactions in 30S ribosomal subunits: folding and function of 16S rRNA. *Science*, **244**, 783–790.
39. Draper,D.E. (1995) Protein-RNA recognition. *Annu. Rev. Biochem.*, **64**, 593–620.
40. Culver,G.M., Cate,J.H., Yusupova,G.Z., Yusupov,M.M. and Noller,H.F. (1999) Identification of an RNA-protein bridge spanning the ribosomal subunit interface. *Science*, **285**, 2133–2136.
41. Champney,W.S. (1980) Protein synthesis defects in temperature-sensitive mutants of Escherichia coli with altered ribosomal proteins. *Biochim. Biophys. Acta*, **609**, 464–474.
42. Yusupov,M.M., Yusupova,G.Z., Baucom,A., Lieberman,K., Earnest,T.N., Cate,J.H. and Noller,H.F. (2001) Crystal structure of the ribosome at 5.5 Å resolution. *Science*, **292**, 883–896.
43. Maisnier-Patin,S., Berg,O.G., Liljas,L. and Andersson,D.I. (2002) Compensatory adaptation to the deleterious effect of antibiotic resistance in Salmonella typhimurium. *Mol. Microbiol.*, **46**, 355–366.
44. Cornish-Bowden,A. (1985) Nomenclature for incompletely specified bases in nucleic acid sequences: recommendations 1984. *Nucleic Acids Res.*, **13**, 3021–3030.